Taylor & Francis
Taylor & Francis Group

Molecular Alignment of Axially-Symmetric Sheared Polymer Network Liquid Crystals

Yung-Hsun Wu
Yi-Hsin Lin
Ju-Hyun Lee
Hongwen Ren
Xiangyi Nie
Shin-Tson Wu
College of Optics and Photonics, University of Central Florida,
Orlando, Florida, USA

An axially-symmetric sheared polymer network liquid crystal (AS-SPNLC) device is demonstrated and its performances characterized. The formation mechanism of the AS-SPNLC is investigated by observing the dynamic pattern change of the structure during the fabrication process. We also analyze the structure from the electro-optic properties and then construct a simulation model to explain the observed phenomena. Several potential applications, such as tunable-focus negative lens and spatial polarization converter, are discussed.

1. INTRODUCTION

An axially-symmetric liquid crystal (LC) structure can be used as a wavelength selection Fabry-Perot filter and a spatial polarization converter. A particularly attractive feature of the axially-symmetric LC structure is its polarization independence because the LC directors are oriented symmetrically in the radial directions. Therefore, we can use it as an optical device which is insensitive to the polarization change [1]. Besides, there is an emerging interest in developing the

space-variant polarized light with axial symmetry [2–4]. Several approaches for achieving this kind of spatial polarization characteristic have been explored. One approach uses the interference of two linearly polarized beams [5]. The major shortcoming of this method is the relatively low light efficiency and complicated fabrication process. Others use special LC cells with circularly rubbing [2,3] or subwavelength gratings [4] to realize the radially or azimuthally polarized light. However, these approaches require a complicated fabrication procedure such as circular rubbing or micro-fabrication process.

To provide a better solution, we have proposed an axially-symmetric sheared polymer network liquid crystal (AS-SPNLC) [6,7]. This structure has attractive features such as fast response time and polarization independence. However, the physical mechanism and structure formation are not yet completely understood. In this paper, we explore the formation processes of an AS-SPNLC structure. By observing of the pattern change of the sheared polymer network liquid crystal (SPNLC) structure, we investigate the formation mechanism of the AS-SPNLC. Besides, through analyzing the structure of the AS-SPNLC, we construct a 3-dimensional model to explain the observed phenomena. The simulation results agree well with experiment. The AS-SPNLC can be used as a tunable-focus negative lens and a spatial polarization converter.

2. SAMPLE FABRICATION

To prepare a PNLC cell, we mixed $15 \, \text{wt}\%$ of a photopolymerizable monomer (Norland optical adhesive NOA65) in a commercial Merck E7 LC mixture. The mixed LC and monomer was sandwiched between two ITO (indium-tin-oxide) glass substrates separated by two stripe mylar spacers. The cell gap was controlled at $\sim 9 \, \mu\text{m}$. To polymerize the LC cell, a two-step UV curing process was adopted [8,9]. In the first step, the LC cell was illuminated to a UV light ($\lambda \sim 365 \, \text{nm}$, $I = 50 \, \text{mW/cm}^2$) for $15 \, \text{min}$ at $T = 110°C$, which is higher than the clearing temperature of E7 ($\sim 60°C$). In the second step, the cell was cured in the same condition but at $20°C$. Since the ITO glass has no surface treatment, the LC domains are randomly distributed so that the cell appears translucent after UV curing. Applying a shearing force along the center of the top substrate while keeping the bottom glass substrate fixed stretches the entangled polymer networks and suppresses the light scattering completely [8,9]. The sheared PNLC cell is highly transparent at $\lambda > 600$ nm. However, if the shearing force is off-axis and the shearing torque is large enough, the polymer
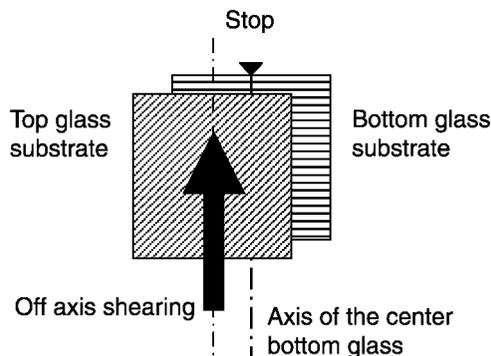
FIGURE 1 Illustration of the off-axis shearing of a SPNLC cell.

networks begin to contract and form an axially-symmetric pattern owing to the restoring force. For example, Figure 1 shows the off-axis shearing of the top glass substrate. The applied shearing force is not along the center of the bottom substrate which is fixed by a stopper. The extra torque results in the polymer network contraction and causes liquid crystal molecules to form the axially symmetric pattern. To control the radial SPNLC patterns, we employed a precise motor motion system (Newport ESP-300) to control the initial acceleration, shearing speed, deceleration, and total shearing distance. The shearing conditions are listed as follows: acceleration $= 10\,\mathrm{mm/s^2}$, speed $= 2.5\,\mathrm{mm/s}$, deceleration $= -10\,\mathrm{mm/s^2}$, and shearing distance $\sim 150\,\mu\mathrm{m}$. To prevent the sheared LC directors from relaxing back, the peripherals of the cell were sealed by a UV adhesive. All our measurements were performed using the sealed LC cell. No noticeable performance change was detected before and after the sealing.

Figure 2 shows the primitive structure of the axially-symmetric sheared polymer network liquid crystal (AS-SPNLC). After the shearing process, the LC directors align toward the center of the pattern. Polymer network forms a radial structure and constrains the LC directors within a circle. The screen shows the image of the AS-SPNLC structure under the crossed polarizers. The black cross is caused by the passing light whose polarization direction is perpendicular to the transmittance axis of the polarizer or analyzer. In order to verify the axially symmetric properties of the SPNLC structure, we rotated the polarizer/analyzer pairs from $0°$ to $360°$ while keeping them crossed. In principle, we could fix the polarizer and analyzer but rotate the sample. The former method is preferred because it keeps the laser beam at the same spot of the sample. Experimental
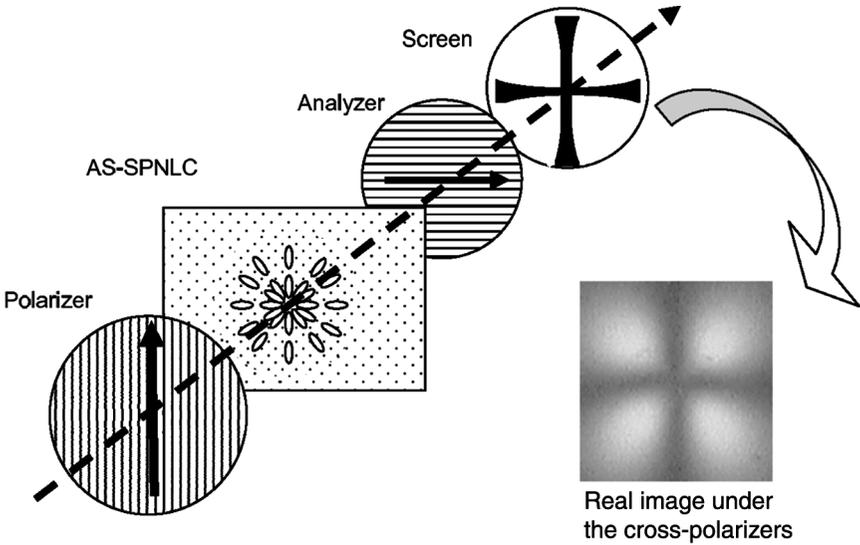
FIGURE 2 SPNLC structure observed under crossed polarizers.

error due to nonuniformity of the sample can thus be ruled out. The experimental results show that the crossed-hair patterns rotate in correspondence of the polarizer/analyzer rotation. The output is identical, independent of the rotation angle of the incident light polarization. This observation confirms that the LC directors indeed are axially symmetric.

3. FORMATION OF THE AS-SPNLC

To understand the pattern formation of the AS-SPNLC, we use a vertical alignment (VA) SPNLC cell as an example. Compared to the non-rubbing sample with scattering conditions, the VA SPNLC is easier to investigate the formation process. In order to enhance the formation phenomena of the AS-SPNLC, we fabricated the VA SPNLC by a quick UV exposure (~ 15 sec). After UV curing process, the VA cell is scattering-free and looks quite transparent. When viewed between crossed polarizers at $V_{rms} = 0$, the cell appears black. This is because of the good vertical alignment of the liquid crystal cell. To observe the AS-SPNLC formation *in situ*, we applied a shearing force to the top glass substrate while keeping the bottom one fixed. Figure 3(a) shows the AS-SPNLC formation while slightly pushing the lower position of the top glass substrate. Under the cross polarizer, we observed several
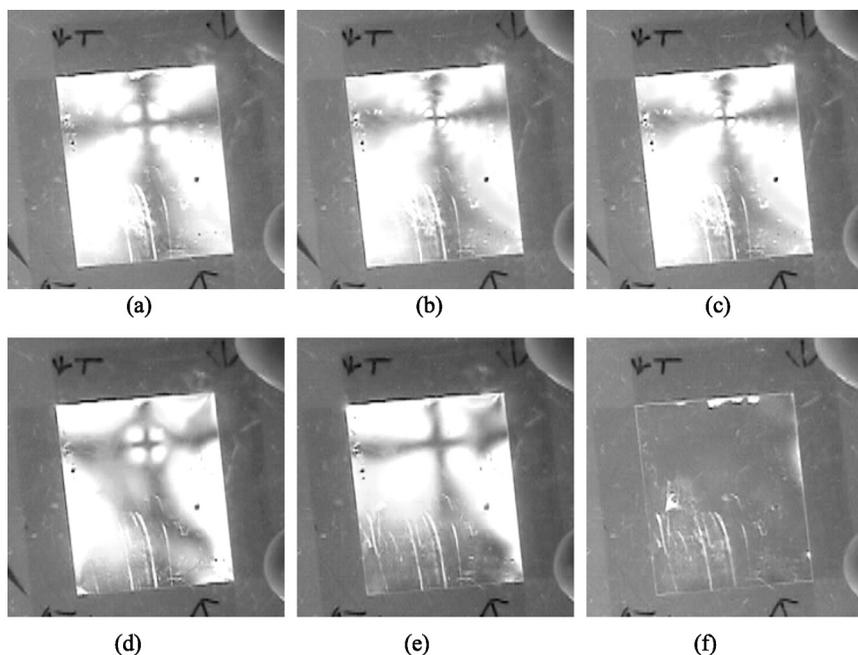
FIGURE 3 (a)–(f) A sequential change of the pattern while pushing the top glass substrate.

concentric rings with a black cross bar in the middle. Each ring represents a 2π phase difference to the adjacent one. The more rings means the larger phase difference between the center and the outmost edge. The black cross bar is caused by the traversed light whose polarization direction is perpendicular to the transmission axis of the polarizer or the analyzer.

Figure 3(a)–(f) show a sequential pattern change VA SPNLC cell before and after pushing the top glass substrate. The number of the rings increases when we push the glass substrate. The increment of the rings implies that more and more liquid crystal molecules tilt away from the vertical alignment because of the external shearing force. The larger tilt angle means the shearing force is stronger and the produced phase difference is larger. The pattern shows the gradient distribution of the phase retardation from the center to the outer ring of the SPNLC structure. The different phase retardation in each position at $V_{rms} = 0$ represents the different LC alignment in the initial state. The larger phase retardation implies a smaller pretilt angle, defined between the optic axis of the LC director and the horizontal direction. After releasing the shearing force of the top glass substrate,
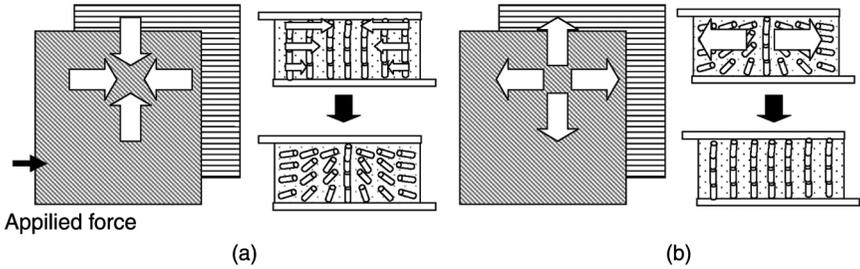
FIGURE 4 Illustration of external force and movement of the liquid crystal directors (a) initial state, and (b) relaxed state.

the AS-SPNLC relaxes back to the homeotropic state so that the phase difference around the pattern vanishes and the rings disappears. To summarize our experimental observation, we saw the liquid crystal directors tilt down from outside to center and relax back to the vertical alignment.

Figure 4 shows the illustration of external force and the movement of the liquid crystal directors. Based on the observation, the liquid crystal molecules receive the external forces from outside toward the center. Hence, the alignment of the liquid crystal molecules is axially symmetric. Figure 4(a) shows the cross-section of the LC director distribution from side view. The gradient force distributes from the top to the bottom of the glass substrate. The liquid crystal directors near the top substrate receive a stronger external force causing a smaller pretilt angle. In contrast, the bottom part receives a weaker force causing a larger pretilt angle. Thus, it forms a hybrid structure, meaning the pretilt angle gradually increases from the top to the bottom glass substrate. Figure 4(b) illustrates the LC director's redistribution after the shearing force is released. The AS-SPNLC relaxes back to the homeotropic state due to the intrinsic elastic force of the liquid crystal directors.

The external force causes the distortion of AS-SPNLC cell. Figure 5 shows an example of the bulk distortion. The surface of the bulk is warped by this external force. To simplify the model, we consider AS-SPNLC as a bulk with elasticity. The top substrate exerts torsion to the bulk molecules when we apply a tangential force to the cell. Figure 6 shows the top view and side view of the distortion. The top glass substrate slightly rotates if we apply an off-axis force. Then, the AS-SPNLC will be distorted while the bottom glass substrate is fixed. A normal stress to the surface is generated while the bulk is distorted. This normal stress has a gradient distribution from the top to the bottom and toward the center. Therefore, the liquid crystal
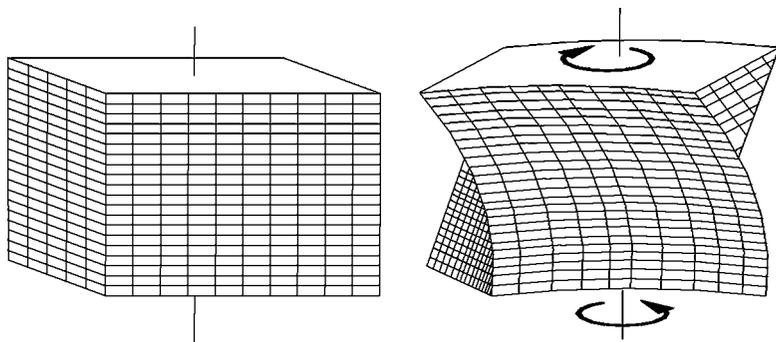
FIGURE 5 An example of the bulk distortion.

directors are reoriented inside the bulk and followed the direction of this external force.

4. EXPERIMENT AND RESULTS

Figure 7 shows the polarization independence of the AS-SPNLC structure. To verify the polarization independence, we measure the voltage-dependent transmittance curves (V-T curve) under three different rotation angles of the crossed polarizers. The input light ($\lambda = 632.8$ nm) was expanded and collimated to 10 mm to cover the central portion of the LC sample. The diameter of the whole sample is ∼20 mm. The reason we narrow down the aperture size to 10 mm is because the central part has better LC alignment and less defects. The V-T curves were measured at three polarizer angles: $0°$, $45°$, and $90°$. The analyzer is always crossed to the polarizer. As shown in Figure 7, the three V-T curves overlap very well. That means the LC directors are distributed in radial directions, as sketched in Figure 2.
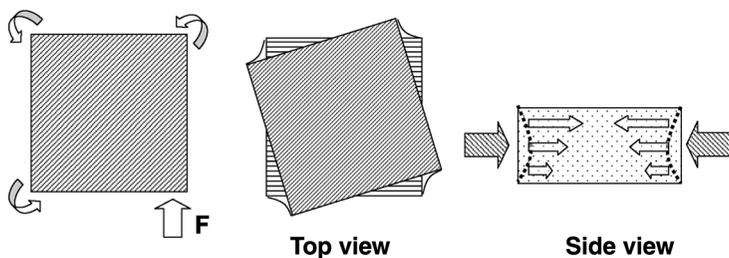
FIGURE 6 Top view and side view of the cell distortion.
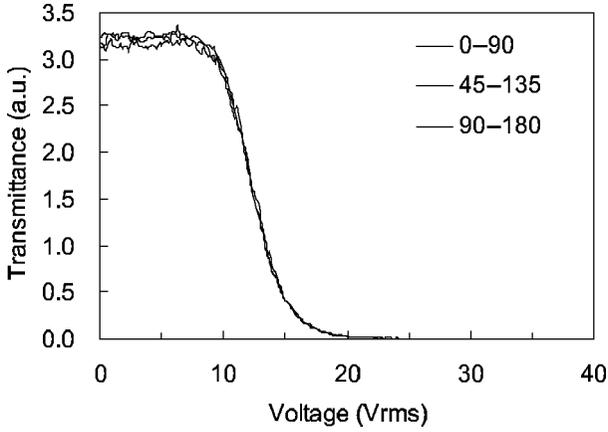
FIGURE 7 Voltage-dependent transmittance of the AS-SPNLC cell. d $= 9\,\mu$m and $\lambda = 633\,$nm.

Figure 8(a) and (b) show the measured response time of the AS-SPNLC. To measure the response time, we applied a $20\,V_{rms}$ at $f = 1\,$kHz square waves to the LC cell. The rise time and decay time are defined from $90 \rightarrow 10\%$ and $10 \rightarrow 90\%$ transmittance change, respectively. The measured optical response times are recorded in the lower traces. From Figure 8(a) and (b), the measured rise time is 0.6 ms and decay time 1.8 ms. From previous studies [8,9], SPNLC exhibit a fast response time because of the small LC domain sizes
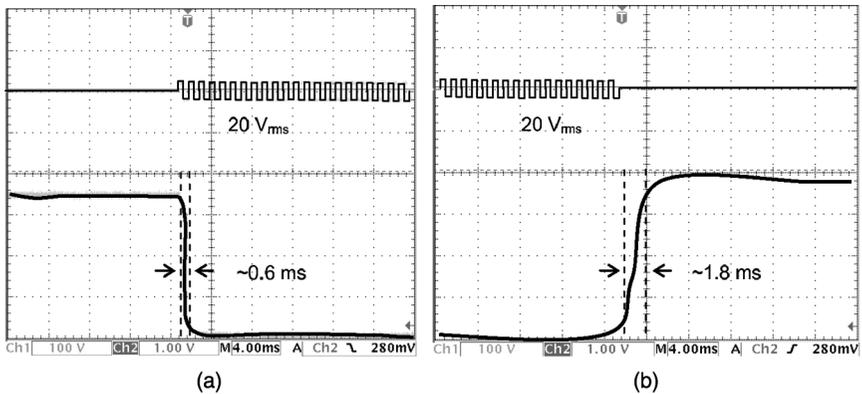
FIGURE 8 Optical response time of a 9-μm AS-SPNLC: (a) rise time, and (b) decay time.
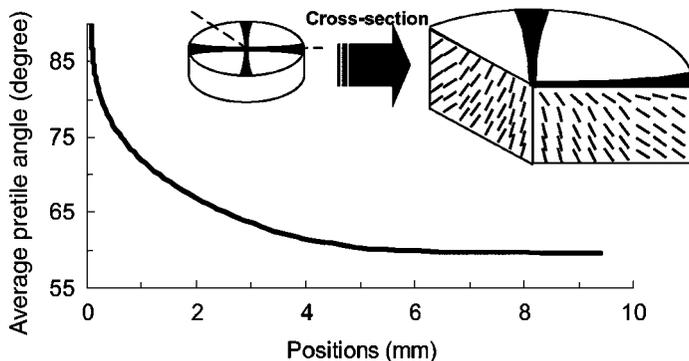
FIGURE 9 Simulated pretilt angle distribution of the AS-SPNLC cell.

and, moreover, the response time is insensitive to the cell gap. Thus, we can use a thick cell gap to gain phase change while still keeping a fast response time. The tradeoff of using a thick LC layer is the increased voltage.

To understand the detailed structure of the AS-SPNLC, we analyze the phase difference at different positions of the pattern. Figure 9 shows the simulated LC tilt angle distribution. At center, the tilt angle is nearly 90°. That means the LC directors are nearly perpendicular to the substrates. This explains why under crossed polarizers the central spot always appears dark. As the radial distance increases, the tilt angle gradually decreases. At each position of the cross-section, the LC directors possess a hybrid structure, i.e., the LC near the top and bottom substrates have different tilt angles. The relatively large tilt angle helps to lower the threshold voltage and the dark state voltage, but the tradeoff is the reduced phase retardation.

Figure 10 plots the measured V-T curves at different radial positions in the pattern. The high driving voltage implies the LC directors are tightly anchored by the polymer networks. It also implies the large elastic constant for the AS-SPNLC structure. Besides, we should also consider the weak surface boundary condition because there is no surface treatment on the glass substrates. The different transmittance of the V-T curve at the initial point represent the different alignment structure at V=0. The higher transmittance means the larger phase retardation. The phase retardation decreases as the position moves toward the center of the pattern.

From Figure 10, the AS-SPNLC has a lower threshold voltage than PNLC. This is because the AS-SPNLC has hybrid LC alignment in each cross-section and the increased tilt angle smears the threshold
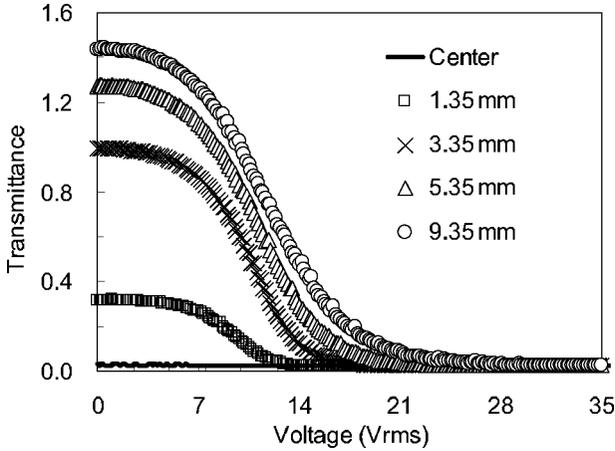
FIGURE 10 Measured V-T curves at different positions of the AS-SPNLC cell.

behavior and lowers the dark state (between crossed polarizers) voltage. On the other hand, a PNLC cell has surface alignment and the employed polymer is quite rigid. As a result, both threshold voltage and operating voltage are relatively high [10].

Figure 11(a) is a series of pictures showing the experimentally observed dynamic image when a voltage is applied to the AS-SPNLC. Based on the measured birefringence, V-T curve, and response

(a)

(b)
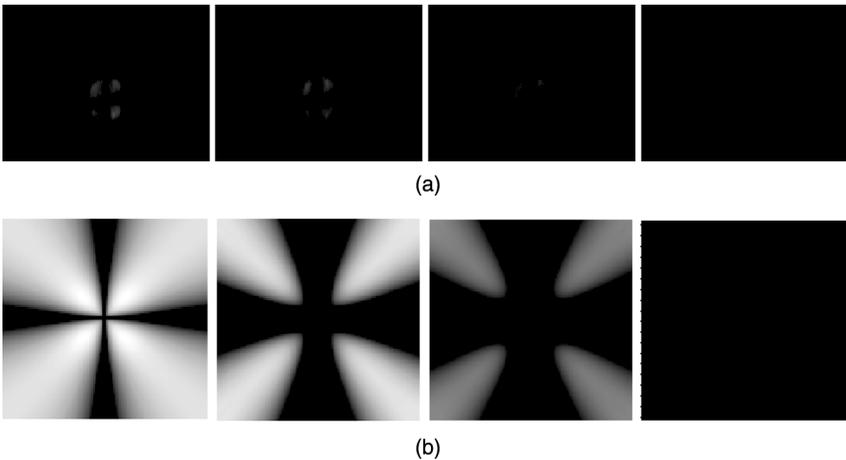
FIGURE 11 (a) Experimental results when a voltage is applied to the AS-SPNLC, and (b) simulated results.

time at different radial positions of the structure, we construct a 3-dimensional model of the LC directors and simulate the dynamic response under crossed polarizers. Figure 11(b) shows the simulated results of the dynamic change when a voltage is applied. The simulation results agree quite well with experiment.

5. DISCUSSIONS

The AS-SPNLC device has potential application as a tunable-focus lens and a spatial polarization converter. For instance, by illuminating with a radially polarized light [11] the AS-SPNLC cell functions like a tunable-focus lens At V = 0, the cell has a natural gradient phase profile from the center to the edge, as shown in Figure 9 so that the lens effect appears. As the voltage increases, the phase profile becomes flatter and the lens effect is gradually vanishing. Since the structure is axially symmetric, the lens performance is independent of the incident light polarization, as shown in Figure 7.

Another interesting application is the so-called spatial polarization converter. For example, we can make a rotationally symmetric half-wave plate using the AS-SPNLC cell if its average dΔn value is equal to $\lambda/2$ [3]. Figure 12 shows the concept of such a polarization converter for the case of P = 2; where P is the polarization order number of the polarized light field [3]. In Figure 12 (a), we illuminate a linearly polarized light to this device. The rotationally half-wave plate shown in Figure 12 (b) would rotate the linearly polarized light to a different angle in each position. This is because the $\lambda/2$ wave plate in each position rotates the linearly polarized light to twice the angle which
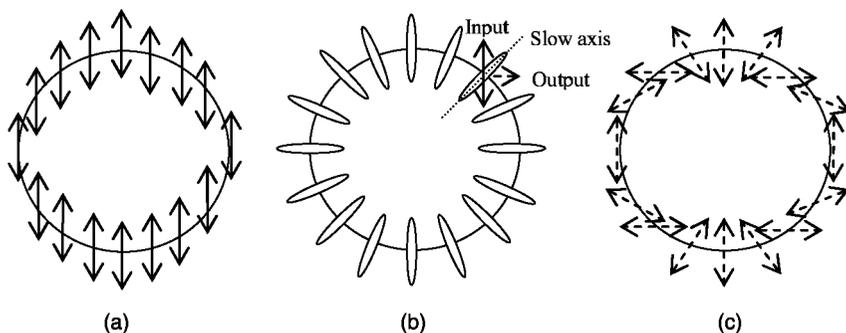
FIGURE 12 (a) Incident light with vertical linear polarization, (b) rotationally symmetric half wave plate, and (c) output light with polarization P = 2 field.

is between the incoming linear polarized light direction and the slow axis. Therefore, the output polarization, as shown in Figure 12 (c) is converted to a circularly symmetric but linearly polarized light field (P=2). Thus, the proposed AS-SPNLC cell will act as a spatial polarization converter

6. CONCLUSION

We have investigated the formation mechanism of the AS-SPNLC structure. The formation of the axially-symmetric structure is caused by the external force toward the center. This external force is generated by the distortion of the liquid crystal bulk while applying an off-axis torque to the SPNLC. The structure of the AS-SPNLC is also analyzed by measuring the birefringence, V-T curve, and response time at different radial positions of the cell. We also construct a 3D model based on the experimental observation. The simulation results agree well with experiment. This device structure has potential applications for a negative tunable-focus LC lens and a spatial polarization converter.

REFERENCES

[1] Lee, J. H., Kim, H. R., & Lee, S. D. (1999). *Appl. Phys. Lett.*, *75*, 859.
[2] Yamaguchi, R., Nose, T., & Sato, S. (1989). *Jpn. J. Appl. Phys.*, *28*, 1730.
[3] Stalder, M. & Schadt, M. (1996). *Opt. Lett.*, *21*, 1948.
[4] Niv, A., Biener, G., Kleiner, V., & Hasman, E. (2003). *Opt. Lett.*, *28*, 510.
[5] Tidwell, S. C., Ford, D. H., & Kimura, W. D. (1990). *Appl. Opt.*, *29*, 2234.
[6] Wu, Y. H., Lin, Y. H., Ren, H., Nie, X., Lee, J. H., & Wu, S. T. (2005). *Opt. Express*, *13*, 4638.
[7] Wu, Y. H., Lee, J. H., Lin, Y. H., Ren, H., & Wu, S. T. (2005). *Opt. Express*, *13*, 7045.
[8] Wu, Y. H., Lin, Y. H., Lu, Y. Q., Ren, H., Fan, Y. H., Wu, J. R., & Wu, S. T. (2004). *Opt. Express*, *12*, 6377.
[9] West, J. L., Zhang, G., & Glushchenko, A. (2005). *Appl. Phys. Lett.*, *86*, 031111.
[10] Fan, Y. H., Lin, Y. H., Ren, H., Gauza, S., & Wu, S. T. (2004). *Appl. Phys. Lett.*, *84*, 1233.
[11] Nesterov, A. V. & Niziev, V. G. (2000). *Phys. D: Appl. Phys.*, *33*, 1817.